Periodica Polytechnica
Civil Engineering

59(2), pp. 193–208, 2015
DOI: 10.3311/PPci.8099

RESEARCH ARTICLE

Comparison of Experimental and Analytical Results on Masonry Infilled RC Frames for Cyclic Lateral Load

István Haris, *Zsolt* Hortobágyi

Received 29-08-2013, revised 11-07-2014, accepted 13-08-2014

Abstract

The aim of the paper is to give a suggestion to the structural engineers to model masonry infilled reinforced concrete frames. We made several experiments, and developed some numerical models. Our previous papers [12–15] *we showed three different FEM numerical models (equivalent diagonal strut model, orthotropic surface model and "suggested sophisticated model"), and we made a comparison study between the numerical results and the experimental tests in case of monotonic increasing lateral loads. The experiments were continued with cyclic lateral loads. Using the earlier proposed bi-linear σ - ε curve of the masonry infill and the different Young's moduli to model unloading, which are based on EC6, shows good correlation with the test results, but unfortunately these are not enough precise to calculate the size of the areas under the load-displacement curves, so we obtained wrong damage parameters. We suggest a new trilinear σ - ε curve. Using this proposed trilinear σ - ε curve of the masonry infill, which is based on EC6, using the "Suggested sophisticated model" with the equivalent struts of the mortar layer shows good correlation with the experimental test results. Both of the calculated dissipated energies can be calculated in good approximation also before and after the yield point of the infill masonry, thus are already usable to calculate the damage parameter D, which were determined by energy concept. With the help of the damage parameter D, a comprehensive damage-equivalent curve $f(D)$ is suggested to calculate the cyclic degradation of the two-storey, one-bay, masonry infilled RC frames.*

Keywords

masonry infilled RC frames · cyclic lateral load · numerical modelling of infill masonry wall · material characteristics of the masonry infill

István Haris

Budapest University of Technology and Economics, Department of Structural Engineering, Műegyetem rkp. 3, H-1111 Budapest, Hungary
e-mail: haris@vbt.bme.hu

Zsolt Hortobágyi

Budapest University of Technology and Economics, Department of Structural Mechanics, Műegyetem rkp. 3, H-1111 Budapest, Hungary

1 Introduction

Nowadays structural design the influence of masonry infills on the behaviour of reinforced concrete frames subjected to earthquake resistance is very important. The most common effect in Hungary, which could be lateral effect during the lifetime of a building according to the valid standard Eurocode 6 [1], is the wind load, but special attention has been nowadays given to the examination on the lateral cyclic horizontal loading, principally on the seismic vulnerability of the masonry infilled concrete frames. To describe and specify the behaviour of the masonry infilled concrete frames for cyclic lateral loading an experimental research was started at BME in Hungary. At the beginning different finite element models had been worked out [12, 14] to describe the behaviour of the infilled frames under lateral loading. A bilinear stress-strain relationship was suggested for the masonry wall, to take into consideration the infills in the RC skeleton. The first experimental test series (9 pieces) and results had been engaged in the examination of the monotonic increasing laterally loaded infilled RC frames [13]. Experimental and different analytical results were compared in [15]. As the next step, the cyclic laterally loaded specimens (6 pieces) were executed and tested [16, 17]. The results and conclusions of the monotonic increasing loaded specimens were the basis of the cyclic laterally loaded experiment studies. The effective and useable load histories were defined according to those considerations. The purpose of the executed experimental program was to specify the behaviour of infilled RC frames for cyclic lateral load, especially when the main continuous diagonal corner-to-corner crack is evolved in the infill masonry, called the "yield point" of the masonry [17].

In this article we give useable methods for the designers to how to take into consideration the infill masonry made of "classical" Hungarian solid masonry units and commercially available mortar for cyclic lateral forces according to Eurocode 6 specify with the nowadays available scientific results.

2 Short review

Many analytical and experimental results showed due to changes in stiffness and mass, dynamic characteristic/response

of the whole structure also changes [5, 9, 10, 20, 28]. The infill masonry has an effect on both global and local failure modes, new and unexpected forms of failure could be appeared [31].

After the opening investigations [18, 26, 32–34] because of the imprecision of the elastic theories, the theories of plasticity were started to use [8, 21, 29, 31, 36]. By the evolution of the softwares using in structural design process many analytical and numerical models and results [14, 22, 24, 27, 28] were published. Above all many experimental results also were presented in connection with the masonry infilled steel frames [30, 35] and concrete frames [4, 6, 7, 23].

Much of the publications dealed with the classical "Equivalent diagonal compressed strut model", of course using plastic elements/springs in FEM software to take into consideration the degradation of the infill masonry. Some/several proposes were worked out to model the softening of the masonry, such as hyperbolic-shaped enveloped model [7], or using a short perfectly plastic zone followed by a linear softening branch [6, 19].

The behaviour of the infill masonry before the appearance of the continuous diagonal corner-to-corner crack is significantly diverged from following the yield point [17]. Under the cyclic forces, which are lower than the yield force, the accumulated residual strains, displacements are smaller in each cycle than in the behaviour stage after the yield point.

Accordingly our approach is a little bit different. The constitutive equations of the masonry infills are based on the models were introduced in [14] and [15], but modified by the theories of continuum damage mechanics. In the theory of damage mechanics the main goal is to evaluate the description of the micro cracks due to mechanical loads. We can introduce a new internal variable, called "D" damage parameter [11, 25, 27]. The variable, combined with numerical FEM results, could be utilized in a relatively easy design procedure.

3 Experimental study

The experimental part of the whole research project was already published. The important details and the maden conclusions could be seen in [13, 15–17].

In this article we would like to give only so short review of the main details and results of the executed experimental result, that the numerical models could be verified and understood.

3.1 Test frames

In the experimental part of the study one-third scale, one-bay, two-storey reinforced concrete (RC) frames were used as specimens in the execution of the tests [13]. On the whole 9 specimens were tested; the dimensions and the reinforcements of the concrete skeleton can be seen in Fig. 1. The ratio of one storey infill height (h) and length (ℓ) h/ℓ is 0,595.

The concrete skeletons were prefabricated in a concrete factory with common characteristics of materials (reinforcement and concrete) were used, see in Table 1.

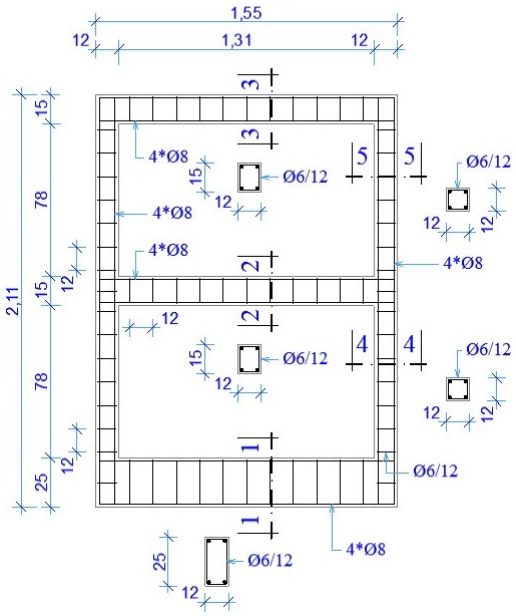

Fig. 1. Dimensions and reinforcements of the test frames

Tab. 1. Classifications of the used materials

Used materials	Classifications	
Concrete	C20/25	$f_{ck} = 20\ N/mm^2$
Steel reinforcement	S500B	$f_{yk} = 500\ N/mm^2$

The RC frame was posteriorly infilled in the laboratory. The used masonry unit was the so-called "classic" solid small brick with dimensions 6.5 * 12 * 25 cm, and each of the elements were cutted into three uniform pieces to take into consideration the scale of the RC test frame, see in Fig. 2.

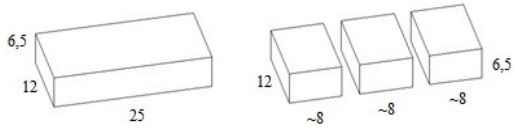

Fig. 2. The "classic" solid small brick in Hungary

The mean compressive strength of the masonry unit (data of the factory) is $f_k = 10\ N/mm^2$. The normalized compressive strength of the cutted units (6.5 * 12 * 8) was calculated by EC6, that is $f_b = 8.57\ kN/mm^2$. The average thickness of both mortar layers was about 3 - 3.5 mm, and the whole surface was covered with mortar. Two different mortars were used in the experiments, Table 2.

Both of the main values of the material characteristic were checked in the laboratory, such as the concrete, the reinforcement and the masonry unit. The difference between the designed and the measured values were similar with each other, except the compression strength of the mortar, see in Table 3.

The infill masonry was continually chocked to the concrete surface with using steel plates, see on Fig. 3.

3.2 Test set-up and procedure

All the fifteen RC frames have the same internal steel reinforcement and divided into five series, each consisting of three

Tab. 2. Classifications of the designed mortars

Classification of mortar	Compr. strength f_m [N/mm^2]
Baumit M30 (M3)	3
Baumit M100 (M10)	10

Tab. 3. Classifications of the executed mortars

Sign of specimen	Executed Class. f_m [N/mm^2]
Km1 - Sp.1.	2,3
Km1 - Sp.2.	2,7
Km1 - Sp.3.	3,3
Km2 - Sp.1.	9,3
Km2 - Sp.2.	8,0
Km2 - Sp.3.	8,5

frames. The first series had no infill masonries, all of the other series had infills. In the second and fourth series the infill masonries were made of the lower compressive strength mortar (M3), as against the third and fifth series, where the higher compressive strength mortar (M10) was used. The second and the fourth series had monotonic increasing lateral, the third and the fifth had in turn cyclic loading, see in Table 4.

3.3 Loading and supporting systems

The one-bay, two-storey reinforced concrete (RC) frames were fixed by complementary steel structures to the concrete slab. The static test loading consisted lateral uniaxial, monotonic increasing loading (V) at the top beam of the frame besides constant (100 kN) vertical load applied on both columns, see on Fig. 4. All of the loadings were applied by using hydraulic jacks. A very rigid external steel frame attached to the specimen was used to prevent any out-of-plane deformations, see also on Fig. 4. The loading and the supporting system was basically the same under the cyclic loading. The only difference was the second lateral hydraulic jack in the countered direction, to be able to create the quasi-static cyclic load histories, see also on Fig. 4.

3.4 Deformation measurements

All deformations were measured by inductive displacement transducers, such as the top drifting under the centre line of the top beam, the relative displacements between the masonry and the concrete, the buckling displacements perpendicular to the equivalent diagonal strut. All the electrical signs were detected and the signals were processed by software and PC. In case of cyclic loading the main differences were that the relative displacements between the masonry and skeleton were measured in symmetric positions, and the buckling displacements were not measured, see on Fig. 5.

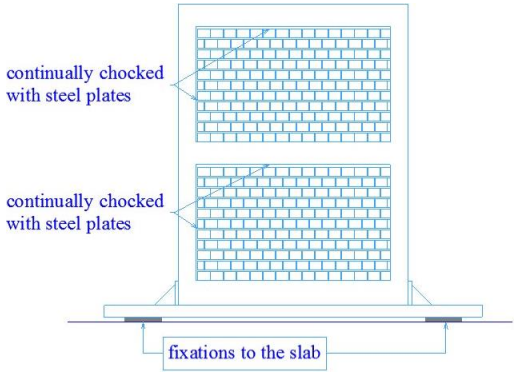

Fig. 3. The infilled frame specimen

Tab. 4. Experimental program

Sign	Test frame set-up	Pieces	Loading set-up
K0	Not infilled	3	monotonic
Km1	Infilled with mortar M3	3	monotonic
Km2	Infilled with mortar M10	3	monotonic
Kc1	Infilled with mortar M3	3	cyclic
Kc2	Infilled with mortar M10	3	cyclic

3.5 Cyclic load histories

The used load histories could be seen on Fig. 6.

3.6 Experimental results

In the followings the test frames are evaluated in terms of load - top displacement. A typical load-top displacement curve is shown up at Fig. 7.

The results of the two test series with the different mortars under monotonic increasing lateral loading are shown at Fig. 8.

The results of the two test series with the different mortars under cyclic lateral loading are shown at Fig. 9.

4 Analytical study

In this main part of the article we present numerical results of different finite element [14] models.

Infill masonry consists of two different materials, the brick and the mortar. The discrete element method (DEM) is the most common used procedure to simulate the contact between the elements. It is computable, but it is very difficult and thus not acceptable to analyse entire buildings.

In numerical analysis of infilled RC frames, the masonry can be modelled by continuum, if the material properties and the sources of non-linearity of the infill are carefully homogenised. Representative volume element (RVE) of masonry is usually used to homogenise the equivalent material properties of masonry. It is a breakable, but very valuable boundary between DEM and continuum model. The present study employs the material as homogenised by the numerical analysis of masonry.

4.1 Elastic and plastic strains

The FEM models and the results usually give/contain the whole lateral response of the structure, therefor the results contain the total strain altogether:

$$\{e^{tot}\} = \{e^{el}\} + \{e^{pl}\} \quad (1)$$

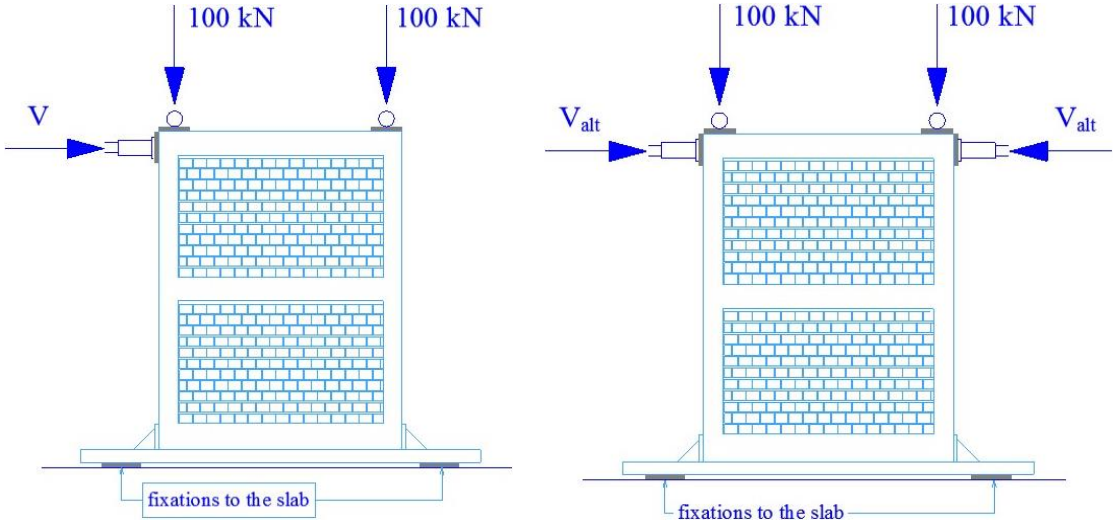

(a) Uniaxial lateral load (b) Cyclic lateral load

Fig. 4. Loading system

where e^{el} elastic strain vector, e^{pl} plastic strain vector.

If we are able to calculate the total and the elastic deformations/strains, the plastic deformations/strains are the followings:

$$\left\{e^{pl}\right\} = \left\{e^{tot}\right\} - \left\{e^{el}\right\} \tag{2}$$

Taken the advantages of Eq. (2), the elastic and total deformations need to be calculated to determinate the plastic deformations. For this the *"Mesh surface model"* and *"Suggested sophisticated model"*, which were defined in [15] (under monotonic increasing lateral load), will be used.

4.2 Material characteristics of the masonry infill

In case of monotonic increasing lateral loading the top displacements of the RC frame were able to be calculated with relatively small error [15] using the suggested bilinear σ - ε curve of the masonry infill. But using the earlier introduced models, the plastic deformations can be calculated as only with the differences of the total and the elastic deformations, Eq. (2). Therefor two different calculations need to be executed.

As an approximation, to model the unloading, different Young's moduli are suggested to be used in the numerical calculations, see in Table 5. Before the yield point of the masonry the Young's modulus (E_{sec}) according to EC6 can be used, but for the closer results after the yield point another modulus need to be applied, namely the initial stiffness ($E_{infill-\beta}$) of the earlier suggested bilinear stress-strain curve [15].

4.3 Degradation and damage

Using a "continuum" model to describe the behaviour of the infill masonry is a common solution [2, 3, 24]. To take into consideration the cyclic degradation, a damage plastic model has been assumed [11, 25, 27]. According to this assumption the analysis of masonry infills is formulated in terms of plasticity with which damaged is associated to the plastic strain.

Continuum damage mechanics are based on the concept of a damage variable. Take a volume element in the continuum, where A is the area of the intersection of one surface and A_d is the effective area of all microcracks and microvoids, than the damage $D_{\vec{n}}$ in this volume element in the direction defined by n can be expressed as:

$$D_{\vec{n}} = \frac{A_d}{A} \tag{3}$$

The damage variable in case of intact element is 0, and 1 in case of total damaged state. In any n direction the $D_{\vec{n}}$ can be approximately the same according to the hypothesis of isotropic damage [11]. In this case the value of the damage can be defined with scalar D in all direction.

$$D_{\vec{n}} \cong D \tag{4}$$

With the normal force F resisted by area A of the volume element, the conventional Cauchy stress is defined as:

$$\sigma = \frac{F}{A} \tag{5}$$

Using the effective (damaged) area A_d instead of the total area A, the effective stress can be represented in the same way:

$$\sigma = \frac{F}{A - A_d} = \frac{\sigma}{1 - D} \tag{6}$$

The hypothesis of strain equivalence states that the behavior of the damaged and the intact material can be described by the same laws [2, 3, 24], if the Cauchy stress is substituted for the effective stress. So the linear elastic behaviour state of a damaged material (in our case this is a brittled crashed material) accordingly can be represented as:

$$\sigma = E\left(\varepsilon^{tot} - \varepsilon^{pl}\right) \tag{7}$$

(a) Measurement points (b) Back-side of the specimen

(c) Measurement system (d) Symmetric measurement points

Fig. 5. Displacement measurement (a-b: monotonic; c-d: cyclic loading)

Tab. 5. Different Young's moduli to model unload

Unload	Before yield point	After the yield point
Young's modulus	E_{sec}	$E_{infill-\beta}$
Could be calculated according to	EC6	suggested bilinear $\sigma - \varepsilon$ curve

using the damage parameter D,

$$\sigma = (1 - D)\, E\left(\varepsilon^{tot} - \varepsilon^{pl}\right) \tag{8}$$

Utilizing the Eq. (8) for the investigated problem, the cyclic crashing/damage can be so taken notice that the elastic strain will be enlarged directly with the rate of the damage. Using this hypothesis the above/earlier introduced numerical models/methods can be utilizable to describe the structural response of the masonry infilled frames for cyclic lateral load before the "yield point" of the masonry with choosing the proper damage parameter D.

Some alternative approaches have been proposed in the literature [8, 19] to estimate the main chracterictic points of the evolution laws of plactic and damage variables according to the thermodinamycs of irreversible processes requires.

In this study to describe the relationship between strain and damage an energy concept will be used combined with the observed and developed behaviour and results of the infill during experimental tests performed in infilled frames subjected to monotonic increasing lateral load and displacement. The following expression will be proposed [7, 19, 25]:

$$E\left(\delta^{pl}\right) = \int_0^{\delta^{pl}} V\left(\delta^{pl}\right) d\delta^{pl} \tag{9}$$

,where V is the external lateral load, and δ^{pl} is the lateral top displacement.

The value of the maximum dissipated energy corresponds to the final fracture is:

$$E\left(\delta^{max}\right) = \int_0^{\infty} V\left(\delta^{pl}\right) d\delta^{pl} \tag{10}$$

Combining Eqs. (9) and (10) the following expression results the damage evolution law, the damage parameter D:

$$D = \frac{E\left(\delta^{pl}\right)}{E(\delta^{max})} \tag{11}$$

After the appearance of the continuous diagonal corner-to-corner crack the original defined continuum divides into two different continuums, henceforward it can appears that the classic continuum conception can be only with difficulty interpreted. Although the divided areas interact with each other, even so definitely are separated and need to be investigated separately. At

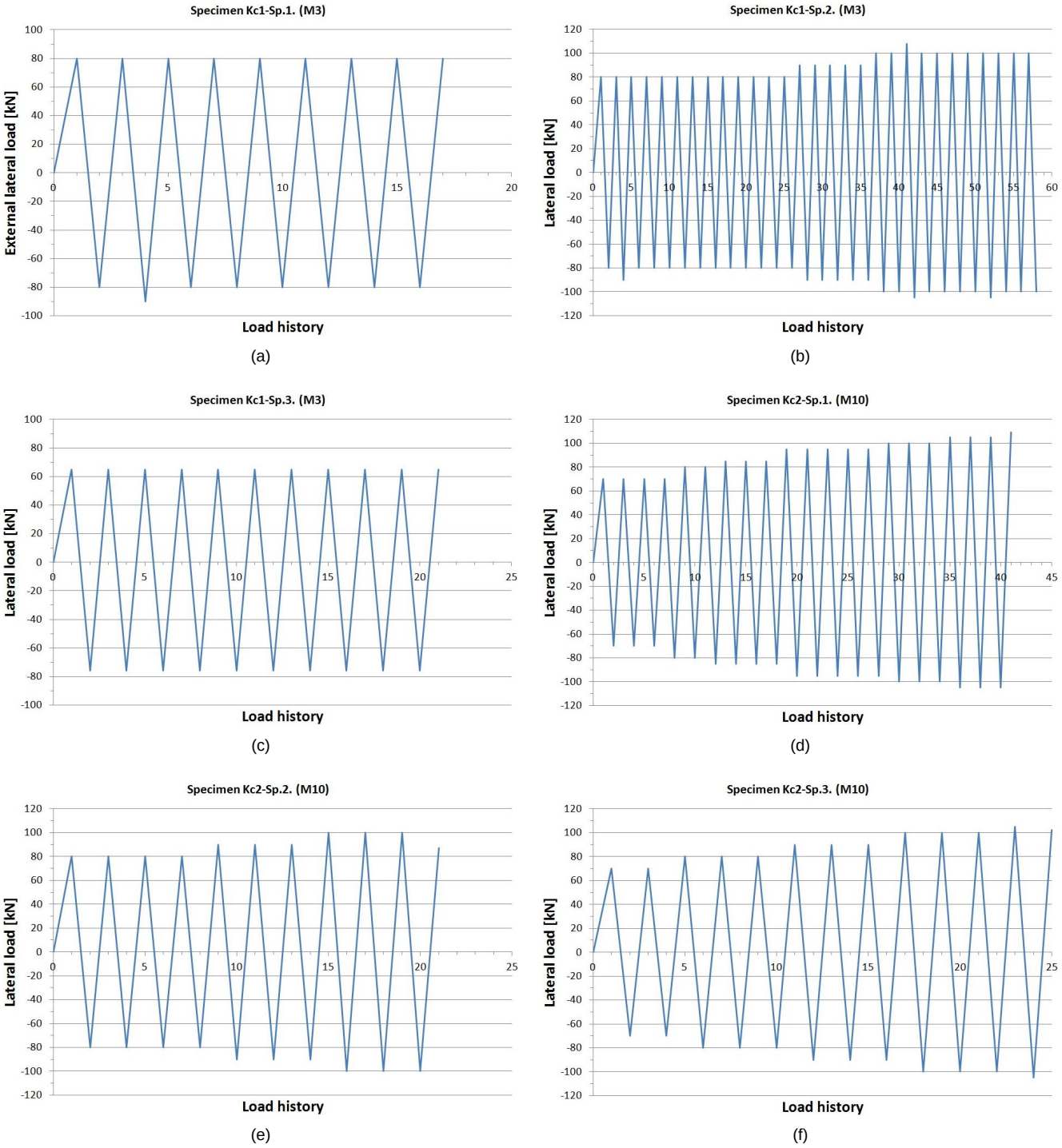

Fig. 6. Cyclic load histories

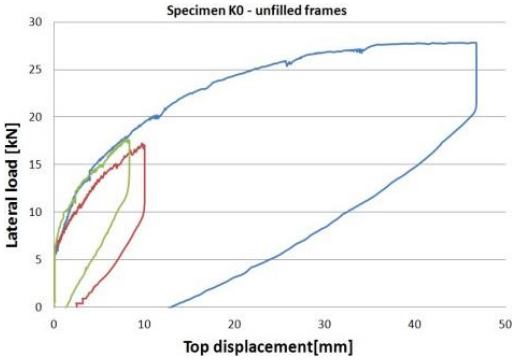

Fig. 7. Load-top displacement curves of the unfilled test frames

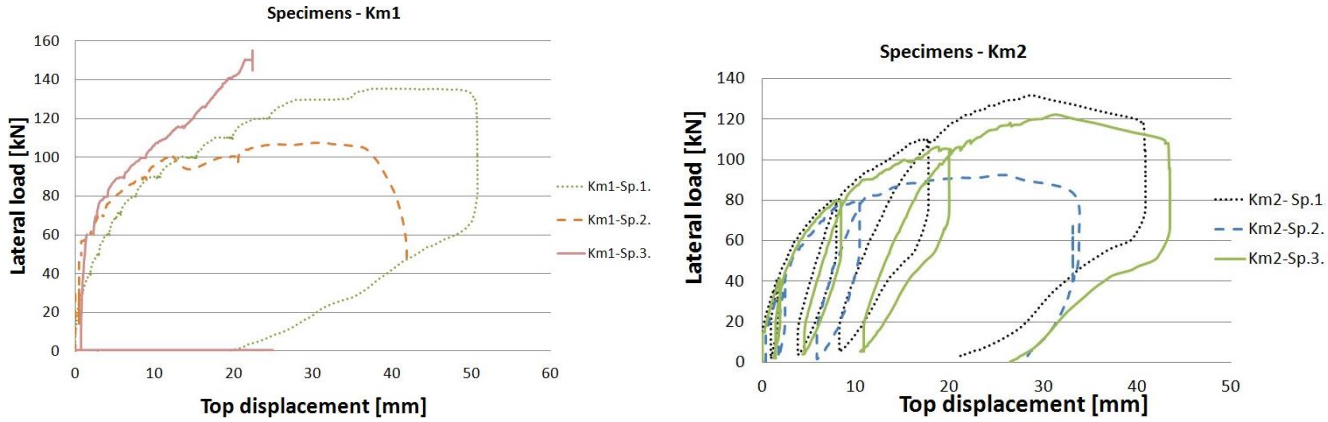

(a) Infilled frames using mortar M3

(b) Infilled frames using mortar M10

Fig. 8. Load-top displacement curve of the infilled test frames under monotonic lateral loading

the same time in our case the general function of the continuum in the numerical investigations is to describe "only" the whole structural response, so the "local" disintegration of the masonry is not a problem. So the numerical simulation can be used after the appearance of the main diagonal corner-to-corner crack in the infill masonry.

Furthermore the *"Suggested sophisticated model"* is able to describe the structural response and the local damages also, because the relative displacements between the different masonry units and rows can appeare, see at Fig. 10.

Using the *"Suggested sophisticated model"* the appearance and the spread of the diagonal crack(s) can be also permanently (in small numerical steps) followed, such like in strut-and-tie models (STM) [24], but in this model the masonry units are defined more sophisticated with shell elements. The corner cracks and damages can be simulated more realistic.

4.4 Determination of the damage parameter

In this study we utilize the experimental results of [13, 16] and [17] to compare with and verify the numerical results received by *"Mesh surface model"* and *"Suggested sophisticated model"*, which were defined in [14] (under monotonic increasing lateral load).

To determinate the damage parameter D the dissipated external potencial energy must be calculated, which in practice means that the size of area under the external lateral force – top displacement curve must be calculated in each load - unload steps.

The comparison of the experimental and the numerical results, in case of monotonic increasing lateral load, can be seen on Fig. 11 and 12.

Using the proposed bi-linear σ - ε curve of the masonry infill and the different Young's moduli to model unloading, which are based on EC6, in an orthotropic surface model *("Mesh surface model")*, or using the *"Suggested sophisticated model"* with the equivalent struts of the mortar layer shows good correlation with the test results, but unfortunately these are not enough precise to calculate the size of the areas under the load-displacement curves, thus the damage parameter D, because:

- by using the *"Mesh surface model"* the deviation of the irreversible plastic top displacements between the experimental and numerical results are high, more than 200%, as it can be seen at Fig. 11 and Fig. 12,
- by using the *"Suggested sophisticated model"* with the equivalent sheared and compressed struts replaced the mortar layer, the computable differences of the irreversible plastic top displacements are under 15% between the numerical and the experimental results before the first corner-to-corner diagonal crack is evolving, after the "yield point" of the infill masonry the differences are under 20%, as it can be seen at Fig. 11 and Fig. 12.

Because of the relatively high inaccuracy of the irreversible

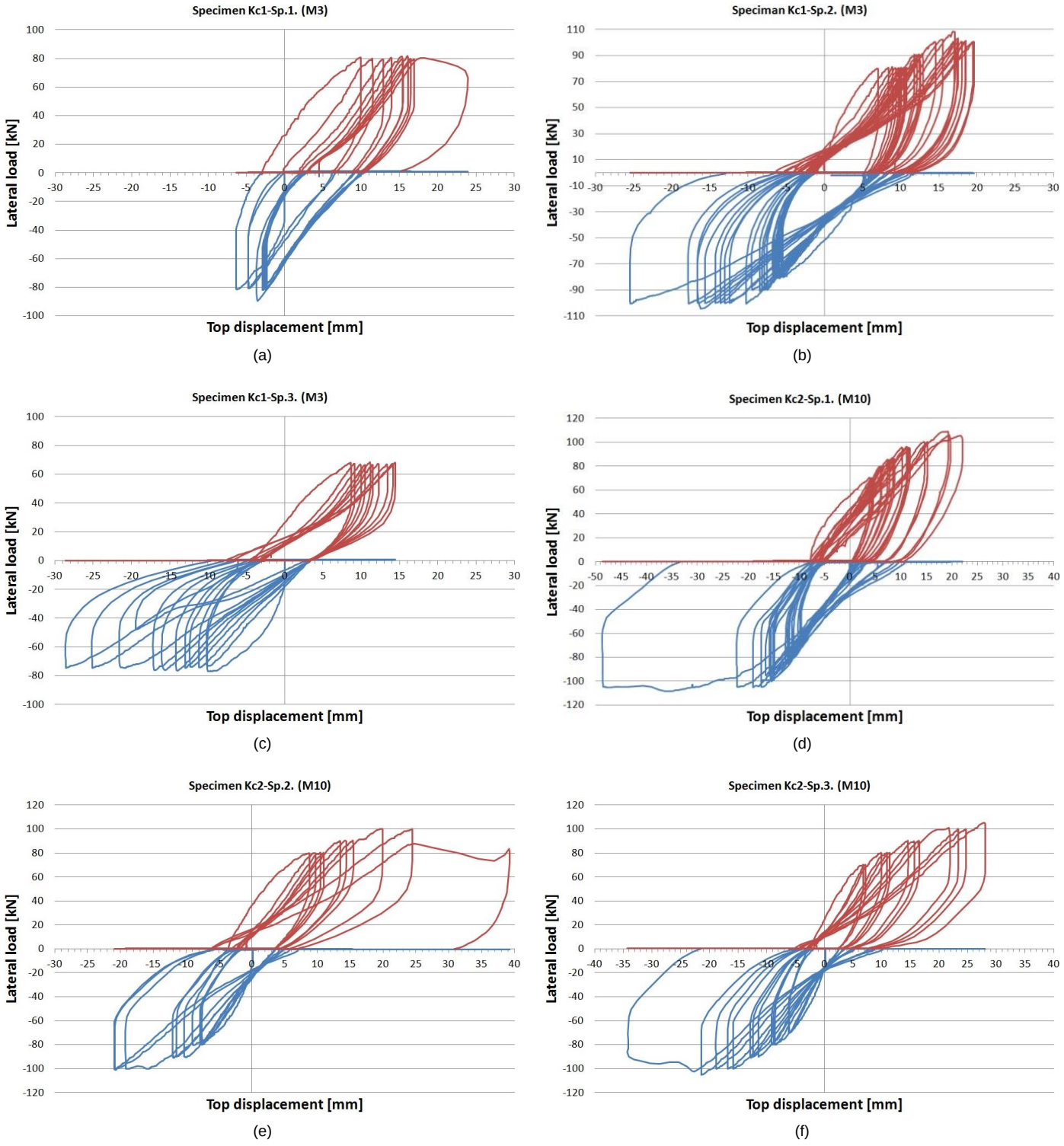

Fig. 9. Load-top displacement curves of the infilled test frames under cyclic loading

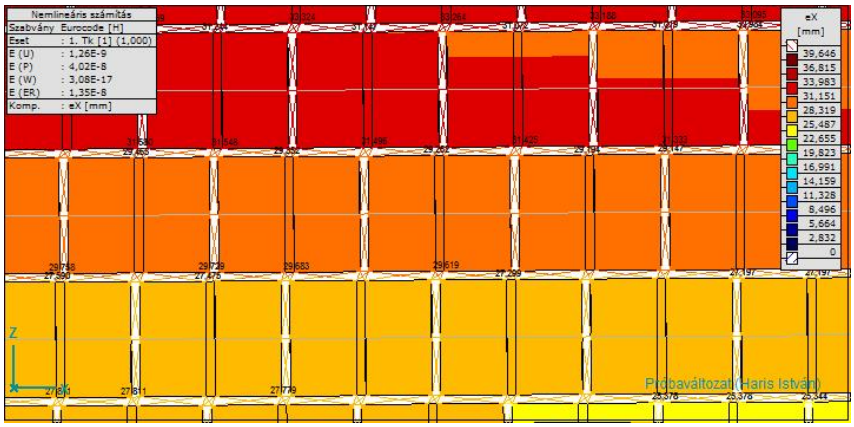

Fig. 10. Relative displacements of the masonry units *("Suggested sophisticated model")*

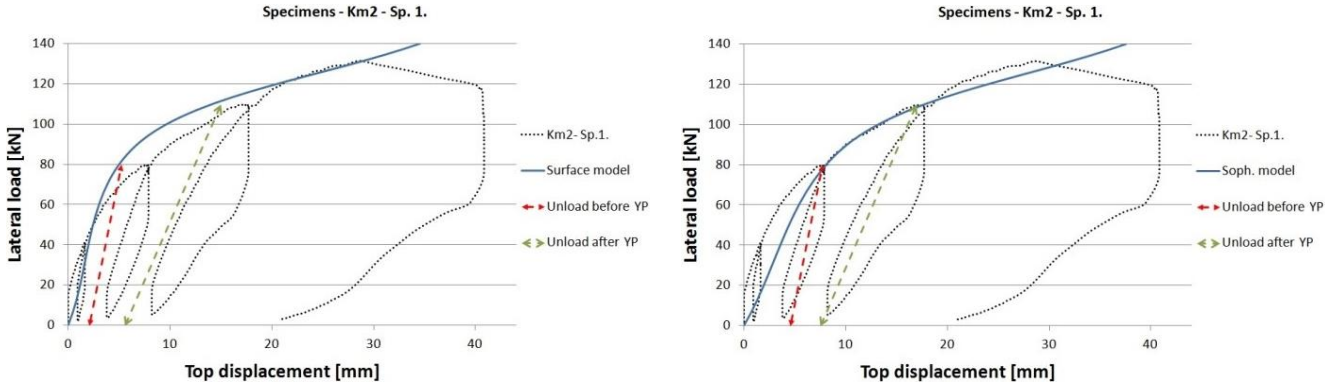

(a) Mesh surface model (b) Suggested sophisticated model

Fig. 11. Load-top displacement curves of the infilled test frames with unload-reload steps *(unload at 80 kN and 110 kN)*

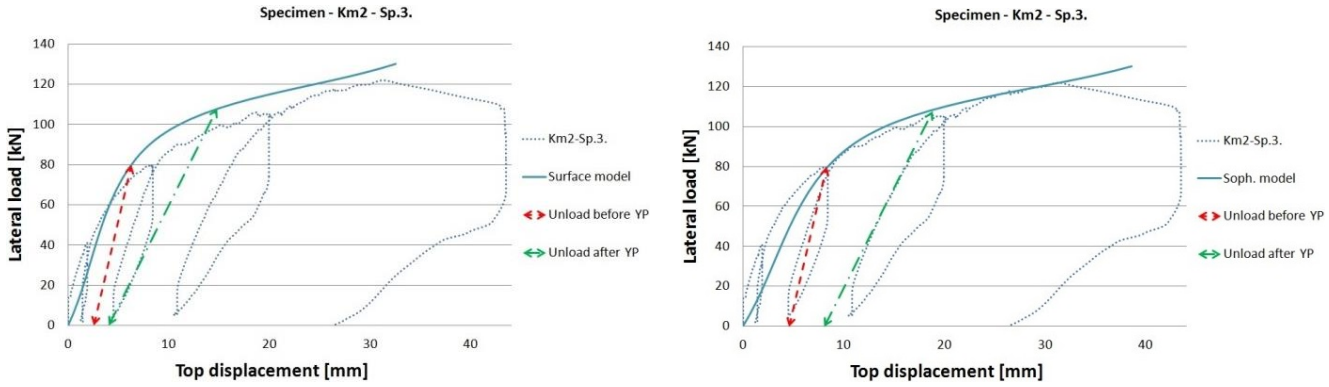

(a) Mesh surface model (b) Suggested sophisticated model

Fig. 12. Load-top displacement curves of the infilled test frames with unload-reload steps *(unload at 80 kN and 110 kN)*

plastic top displacements of the *"Mesh surface model"*, henceforward only the *"Suggested sophisticated model"* will be tried to calculate the size of the areas under the load-displacement curves. The calculatable areas by the *"Suggested sophisticated model"* compared with the experimental results are shown on Fig. 13 and Fig. 14:

The differences of the size of the areas under the curves, of the dissipated energies between numerical and experimental results are shown in Tab. 6:

Tab. 6. Differencies of the sizes of the calculated and measured areas under the curves

Differences	at 80 kN	at 110 kN
Km 2-1	44,63%	35,39%
Km 2-3	44,21%	32,99%

Athough the numerically calculated and the measured top displacements were close to each other using the *"Suggested sophisticated model"* with the bi-linear σ - ε curve of the masonry infill and the differerent Young's moduli to model unloading, but the dissipated energies shows not enough good correlation to use up those in further calculations.

To be able to numerically acceptable describe the cyclic lateral damage of the masonry infilled frames, more specified load-displacement curves must be prepared. The easiest way for this is to specify the usable σ - ε curve of the masonry infill.

4.5 New tri-linear σ - ε curve of the masonry infill

According to EC6 specified with the suggestions of [15], we suggest to use a new σ - ε diagram on theabove mentioned cyclic damage designing method of the lateral loaded masonry infills. A trilinear relation stress-strain diagram could be defined, up to the 40% of the "yield point" (the appearence of the first main diagonal corner-to-corner crack in the masonry) an elastic (E_{sec}) section could be defined in totally accordance with EC6.

$$E_{sec} = 1000 f_k \tag{12}$$

,where f_k is the characteristic compressive strength of the masonry (using general purpose mortar).

After it, another linear elastic line could be defined up to the "yield point" of the masonry infill:

$$f_{infill-\beta} = 0.7 * f_k \tag{13}$$

,where f_k is again the characteristic compressive strength of the masonry.

The perfect plasticity should be neglected, than a monotonic linear decreasing section is suggested, see on Fig. 15.

To model the unloading, the earlier defined Young's moduli are henceforward suggested to be used in the numerical calculations. Before the yield point of the masonry the Young's modulus (E_{sec}) according to EC6 can be used, but for the closer results after the yield point another modulus ($E_{infill-\beta}$) need to be applied:

$$E_{infill,\beta} = \left\{ \frac{1}{E_{infill.0}} cos^4(\beta) + \left[-\frac{2\nu_{0-90}}{E_{infill.0}} + \frac{1}{G_{infill}} \right] cos^2(\beta)\, sin^2(\beta) + \frac{1}{E_{infill.90}} sin^4(\beta) \right\}^{-1} \tag{14}$$

where $E_{infill.0}$ and $E_{infill.90}$ are Young's modulus of the infill masonry in the direction to parallel and normal to mortar bed joints, $E_{infill.90}$ is equal to E_{sec}, ν_{0-90} is Poisson's ratio, G_{infill} is shear modulus. $E_{infill.0}$ could be taken as half of $E_{infill.90}$, and $\nu_{0-90} = 0.25$ [14].

4.6 Approximation of the dissipated energy

The damage parameter D, which has been determined by energy concept, can be again calculated by using the above introduced trilinear stress-strain diagram.

In the interest of the comparability with the earlier introduced results (using the bilinear diagram) the same experimental results will be used for the verification. The specified numerical results using with the new trilinear σ - ε diagram are shown on Fig. 16.

The dissipated energies can be calculated again as the size of the area under the load-displacement curves, see on Fig. 17.

The differences of the size of the areas under the curves, of the dissipated energies between numerical and experimental results using the suggested new trilinear σ - ε curve of the masonry infill are shown in Tab. 7:

Tab. 7. Differencies of the sizes of the calculated and measured areas under the curves

Differencies	at 80 kN	at 110 kN
Sp. Km 2-1	11,19%	0,49%
Sp. Km 2-3	18,26%	3,19%

Using the proposed trilinear σ - ε curve of the masonry infill, which is based on EC6, using the *"Suggested sophisticated model"* with the equivalent struts of the mortar layer shows good correlation with the test results. Both of the calculated dissipated energies can be calculated in good approximation also before and after the yield point of the infill masonry, thus are already usable to calculate the damage parameter D, which were determined by energy concept.

4.7 Cyclic degradation

As it was introduced in the previous chapter, the damage parameter D of a masonry infilled one-bay, two-storey reinforced concrete frame can be numerically calculated in very good correlation by using the proposed trilinear σ - ε curve of the masonry infill and the *"Suggested sophisticated model"* under monotonic increasing lateral external forces.

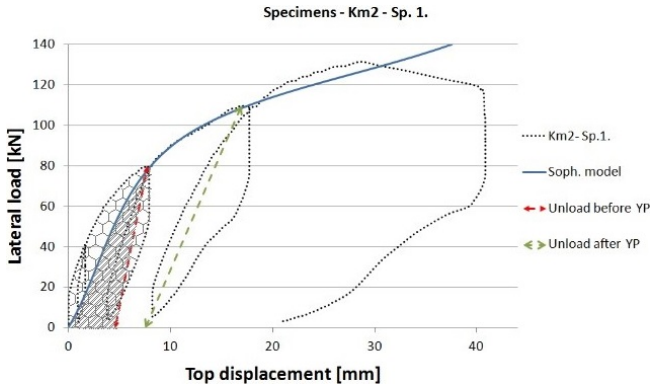

(a) unload at 80 kN

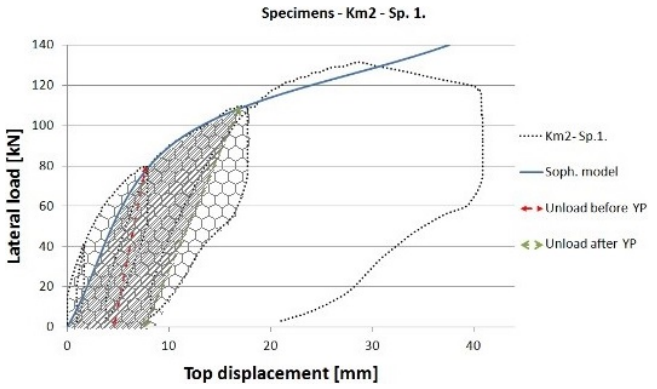

(b) unload at 110 kN

Fig. 13. Areas under load-displacement curve before and after "yield point"

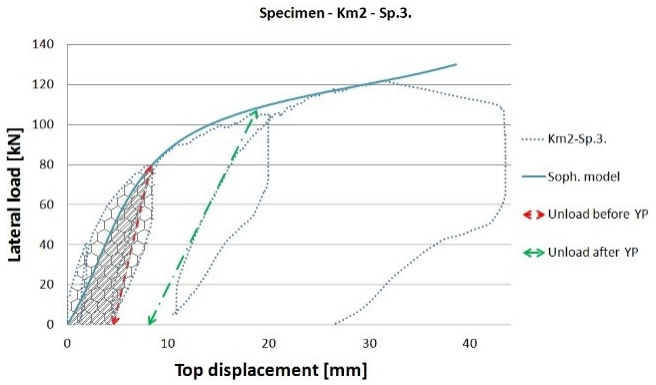

(a) unload at 80 kN

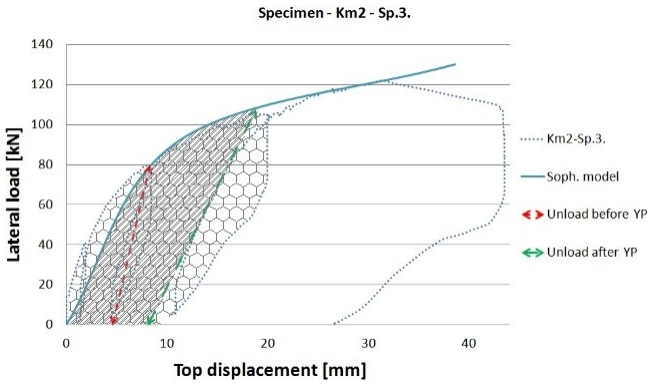

(b) unload at 110 kN

Fig. 14. Areas under load-displacement curve before and after "yield point"

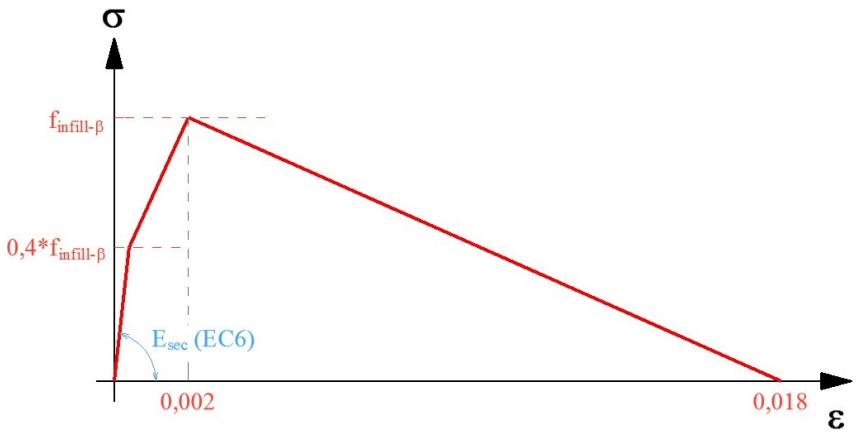

Fig. 15. Suggested new trilinear σ - ε curve of the masonry infill

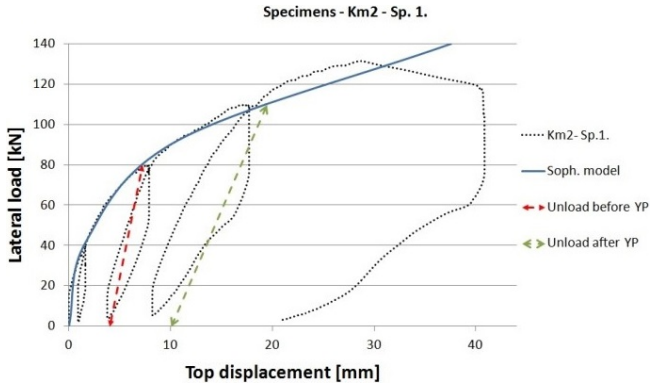

(a) Specimen Km 2-1

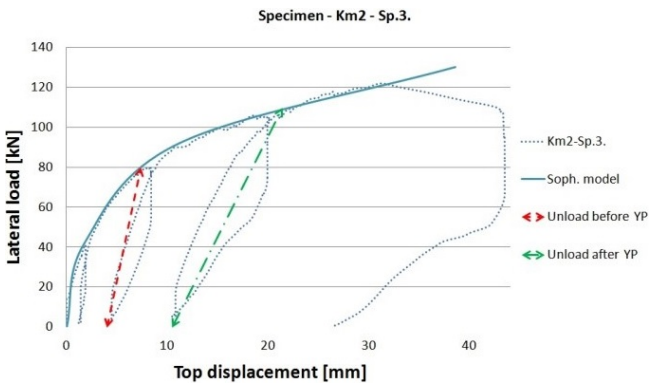

(b) Specimen Km 2-3

Fig. 16. Suggested new trilinear σ - ε curve of the masonry infill

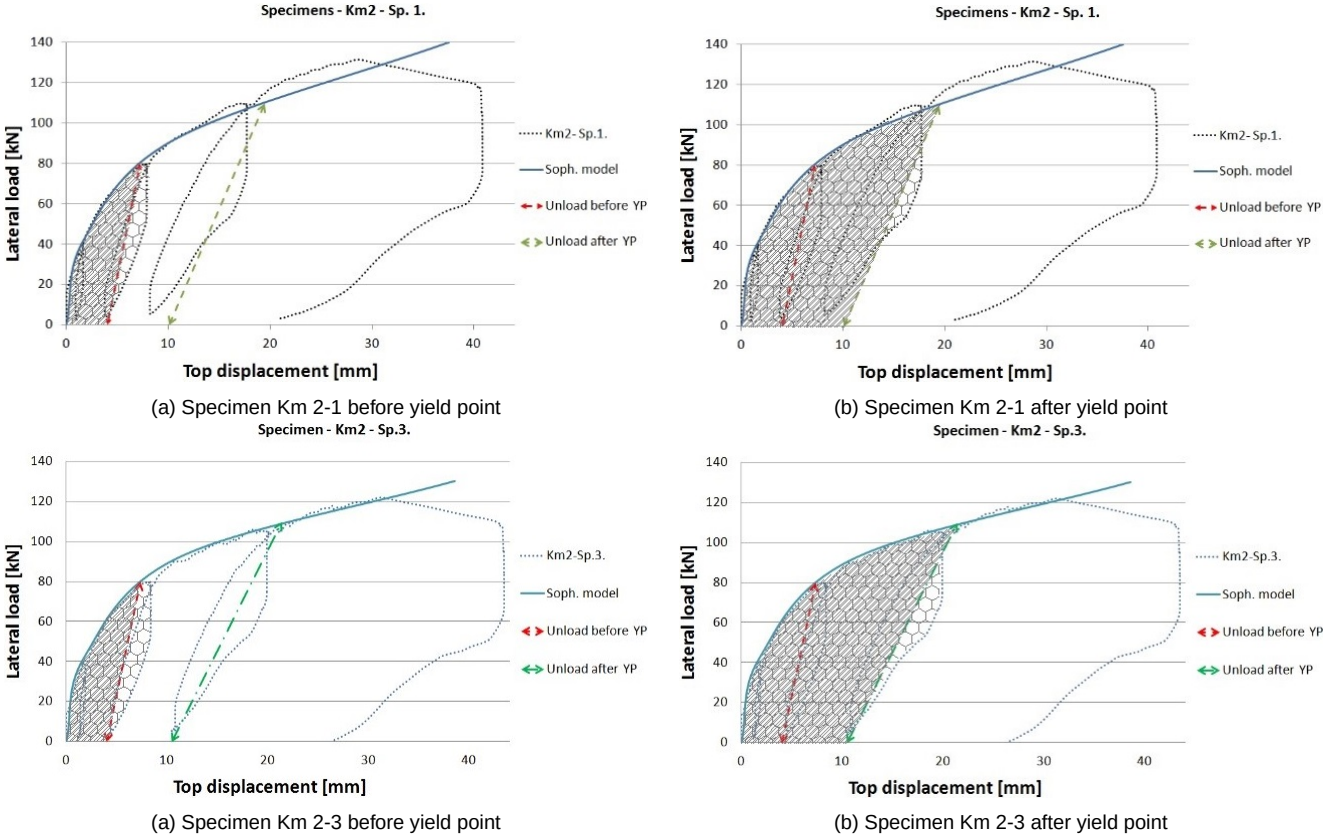

(a) Specimen Km 2-1 before yield point

(b) Specimen Km 2-1 after yield point

(a) Specimen Km 2-3 before yield point

(b) Specimen Km 2-3 after yield point

Fig. 17. Load-top displacement curves of the infilled test frames with unload-reload steps using the trilinear $\sigma - \varepsilon$ diagram (unload at 80 kN and 110 kN)

Using the suggested Young's moduli to model the unload sections the dissipated energies and the damage parameter can be calculated.

A typical damage parameter – load quotient (V / V_{peak}) curve is shown on Fig. 18.

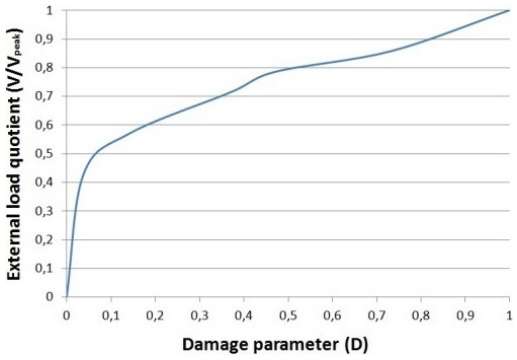

Fig. 18. Typical external load quotient-damage parameter curve

By using the experimental test results of [4, 7, 13, 16, 17], and the own numerical results an $f(D)$ comprehensive damage-equivalent curve, which is depend on the above calculated damage parameter D, can be suggested to take into consideration the whole structural degradation of a masonry infilled one-bay, two-storey reinforced concrete frame.

The suggested a $f(D)$ comprehensive damage-equivalent curve is:

$$f(D) = \frac{1}{2}\left(1 - e^{-\frac{D^3}{2}}\right) \tag{15}$$

,where D is the damage parameter, which is determined by energy concept.

The suggested $f(D)$ comprehensive damage-equivalent curve and the values of the calculated damage parameters by the used test results are shown on Fig. 19.

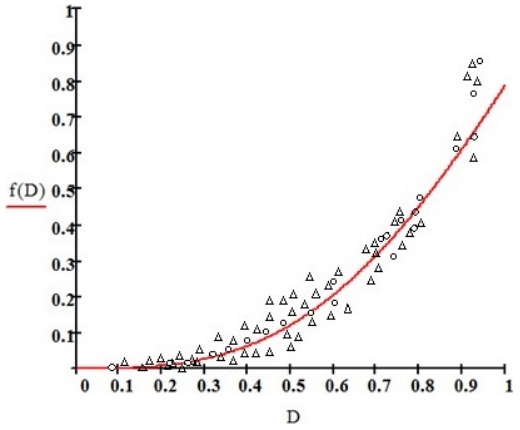

Fig. 19. Suggested comprehensive damage-equivalent curve

,where Symbol "O" is the calculated damage parameter by using own test results, and Symbol "Δ" is the calculated damage parameter by using the test results of [4] and [7].

Using the value of the suggested $f(D)$ comprehensive damage-equivalent curve and Eq. (8), the whole structural degradation can be taken into consideration by the following:

$$\sigma = (1 - f(D))\, E\left(\varepsilon^{el}\right) \tag{16}$$

Eq. (16) can be used to modify the secant Young's modulus (E_{sec}) of the earlier suggested trilinear σ - ε curve of the masonry infill. So the modified secant Young's modulus (E_D), which contains the structural damage, is the following:

$$E_D = (1 - f(D))\, E_{sec} \tag{17}$$

To be able to model the cyclic degradation of the infilled frame the above mentioned calculation must be repeated by the following flow diagram, see on Fig. 20.

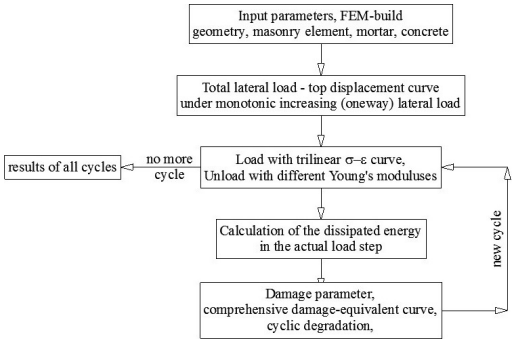

Fig. 20. The flow diagram of the calculation of the cyclic degradation

In view of the effective load history, the external lateral load – top displacement curve of certain load step is calculatable under monotonic increasing lateral load. So thus each of the damage parameter can be calculated. The numerical principle of the degradation of the secant Young's moduli in each load step is shown on Fig. 21.

Either $(i)^{th}$ load-displacement curves can be produced by using the total structural damages $(1 - f(D)_i)$ of all previous cycles:

$$1 - f(D)_i = \prod_{k=1}^{i-1} (1 - f(D)_k) \tag{18}$$

5 Comparison of numerical and experimental results

The comparison of the calculated and the experimental results of Specimen Kc 1-2 is shown on Fig. 22.

The results for the whole load history in case of Specimen Kc2-2 and Kc2-3 are shown on Fig. 23 and Fig. 24.

With the introduced calculation method the deviations of the estimation of the top displacements and the envelope of the cyclic curves show quite good correlation with the experimental results. By the investigation of the above shown figures the following statements could be made:

- Kc 1-2.: the coincidence of the experimental and the analytical results is very good using the suggested trilinear σ - ε diagram for the infill masonry, the comprehensive damage-equivalent curve for the degradation and the suggested sophisticated FEM model.
- Kc 2-2.: in the first cycles of the load history the calculated results are lower than the measured, so the structure has higher stiffness, but after the yield point it has changed, and the calculation shows lower stiffness. Before the yield point of the masonry the biggest deviation is lower than 10%, and after the appearance of the diagonal corner-to-corner contionius crack it is lower than 20%. The coincidence of the experimental and the analytical results is also very good.
- Kc 2-3.: the coincidence of the experimental and the analytical results is again very good. The biggest deviations are less than 10% and 20%, before and after the yield point between the numerical and the experimental results.

Between the calculated and the measured accumulated residual plastic deformations there are relatively big differences, but the envelope curve of both results shows very good coincidence.

The final failure of the infilled frame under cyclic lateral loads dues to happen if the biggest relative top displacement in one cycle is quasi equal to the maximum/failure top displacement could be calculated/measured under monotonic increasing lateral load.

6 Conclusions

The conclusions made below are based on the limited data of the experimental tests and numerical studies of the masonry infilled RC frames. The numerical results of the finite element models of masonry infilled reinforced concrete frames were compared with experimental results.

The two-storey, one-bay RC test frames infilled with masonry showed similar cyclic behaviour, especially the initial stiffness of the frames, the yield point of the masonry infills and the peak lateral loads and deformations were close.

As an approximation, to model the unloading, different Young's moduli are suggested to be used in the numerical calculations. For the more specified results and to be able to calculate the dissipated energy in any point of the load history a new trilinear σ – ε curve were introduced, which gives usable results by applying the *"Suggestes sophisticated model"*. The *"Mesh surface model"* has given relatively big differences, when the size of the area under the load-displacement curve was investigated.

Using the bilinear stress-strain diagram and the mesh surface model is not suggested to model the behaviour of the infill frames under cyclic loads, because the numerical results of the calculated dissipated energies show quite big (~40%) differences. Although the numerical results are not enough close to the experimental results to calculate the dissipated energies, which are necessary to determinate the cyclic degradation, but the bilinear material data and the orthotropic mesh model are still usable to approximate the top displacements of the frame under monotonic increasing loads.

By using the proposed trilinear material characteristics of the infill masonry in the suggested sophisticated FEM model gave extra safe and reliable results to the behaviour of the infilled RC frames under both monotonic increasing and cyclic lateral loads also.

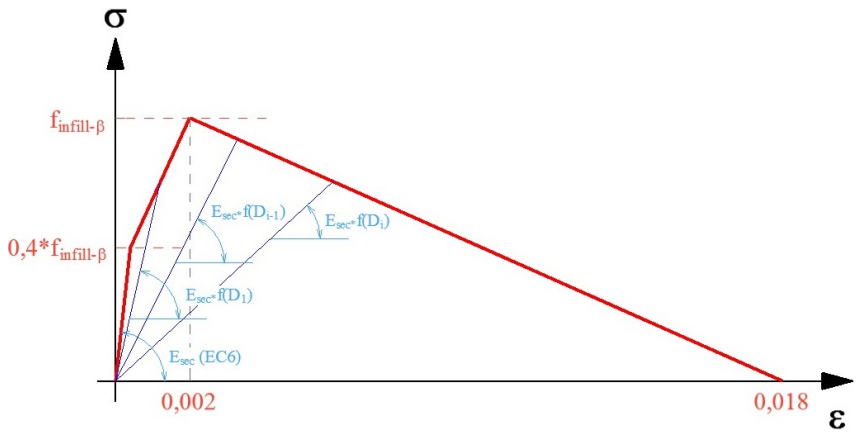

Fig. 21. The modified Young's moduli under cyclic degradation

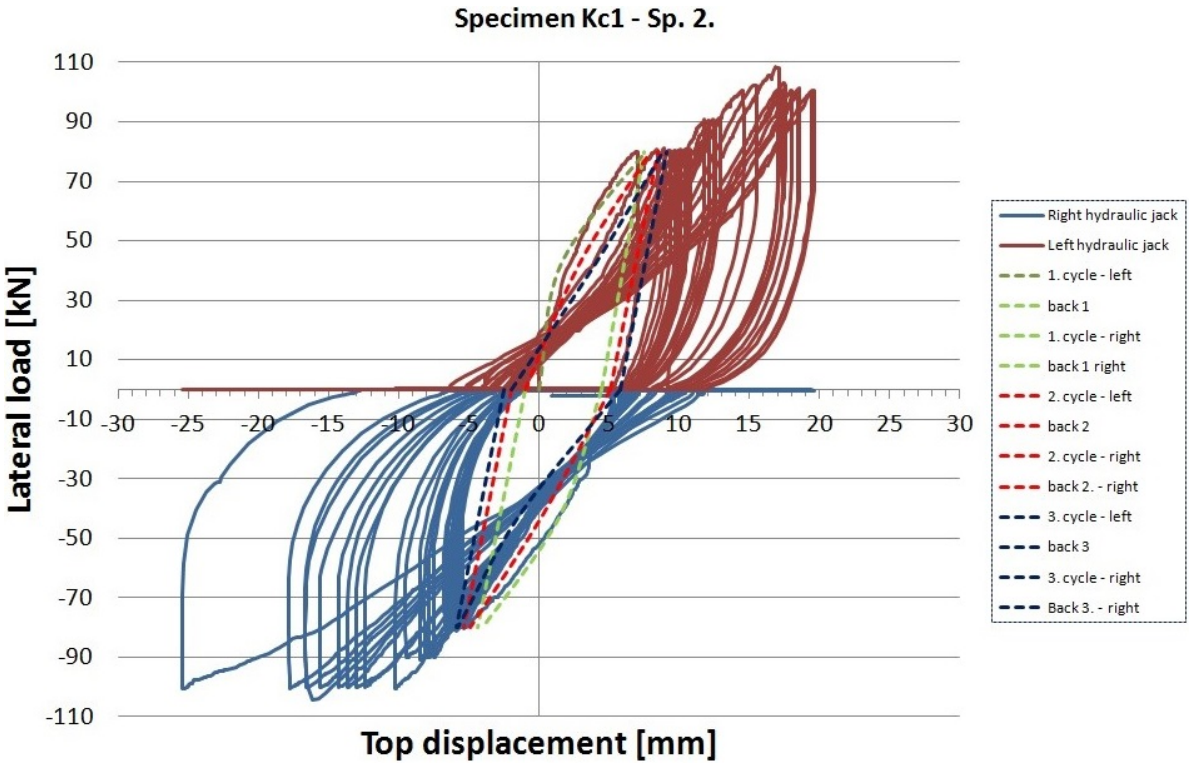

Fig. 22. Comparison of calculated and experimental results of Sp. Kc 1-2

Although this proposed method is more difficulty, and needs a little bit "smarter" softwares, closer results can be presented for the top displacements, already for the determination of the dissipated energies and the damage parameter. By the help of the damage parameter D of the structure, calculated under monotonic increasing lateral load, a comprehensive damage-equivalent curve $f(D)$ was suggested to calculate the cyclic degradation of the two-storey, one-bay, masonry infilled RC frames.

The calculation of any point of a cyclic load history is able to be made by using the proposed calculation method. It is much more complicated, even so probably is usable in design practice. This model gave close numerical results in top displacements to the experimental results. The differences between the experimental and analytical results were under 10% at the stage before and 20% after yield point of the masonry infill.

The final failure of the infilled frame under cyclic lateral loads can be predicted. The collapse will be evolved, if the biggest relative top displacement in one cycle is quasi equal to the maximum/failure top displacement could be calculated under monotonic increasing lateral load.

Using the proposed trilinear σ - ε curve of the masonry infill with different Young's moduli for the unload steps, which are based on EC6, in a suggested sophisticated model shows good correlation with the test results, strangly with the dissipated energies. By using the proposed damage parameter, and the comprehensive damage-equivalent curve the cyclic degradation of the investigated masonry infilled RC frames can be calculated in good approximation also before and after the yield point of the infill masonry, and are already usable to model the behaviour under cyclic lateral loads in the structural engineering.

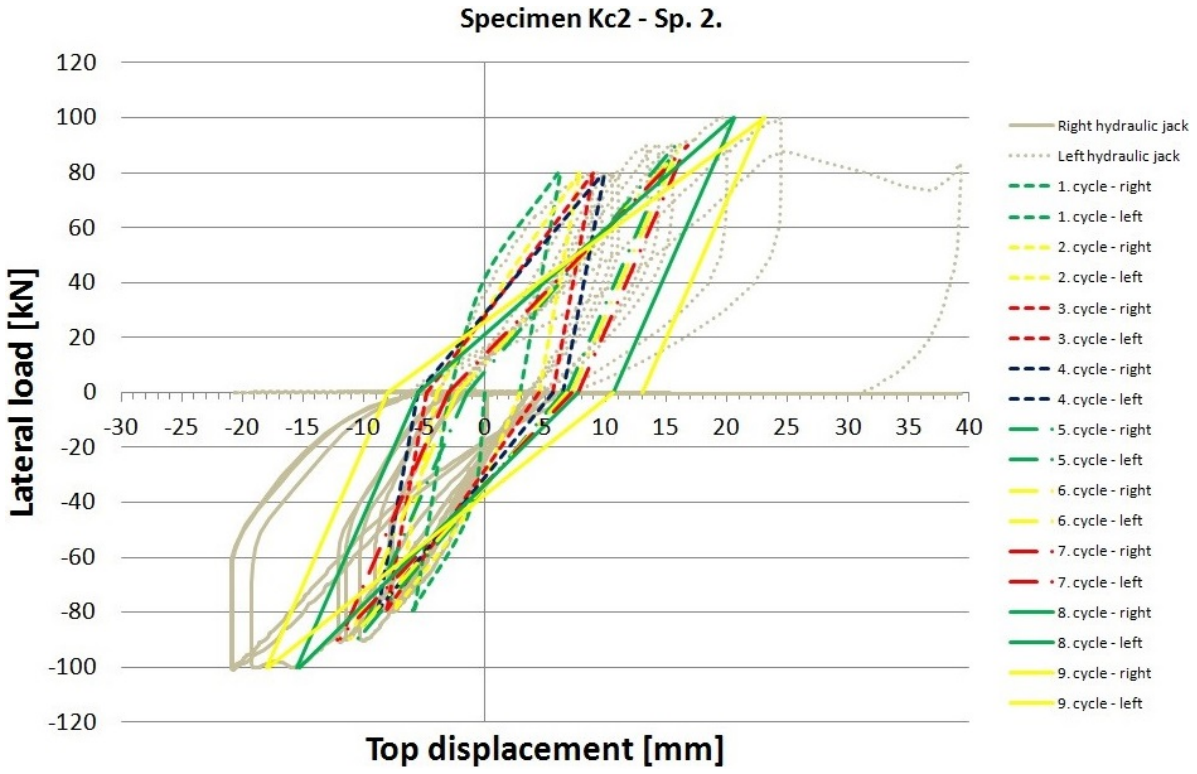

Fig. 23. Comparison of calculated and experimental results of Sp. Kc 2-2

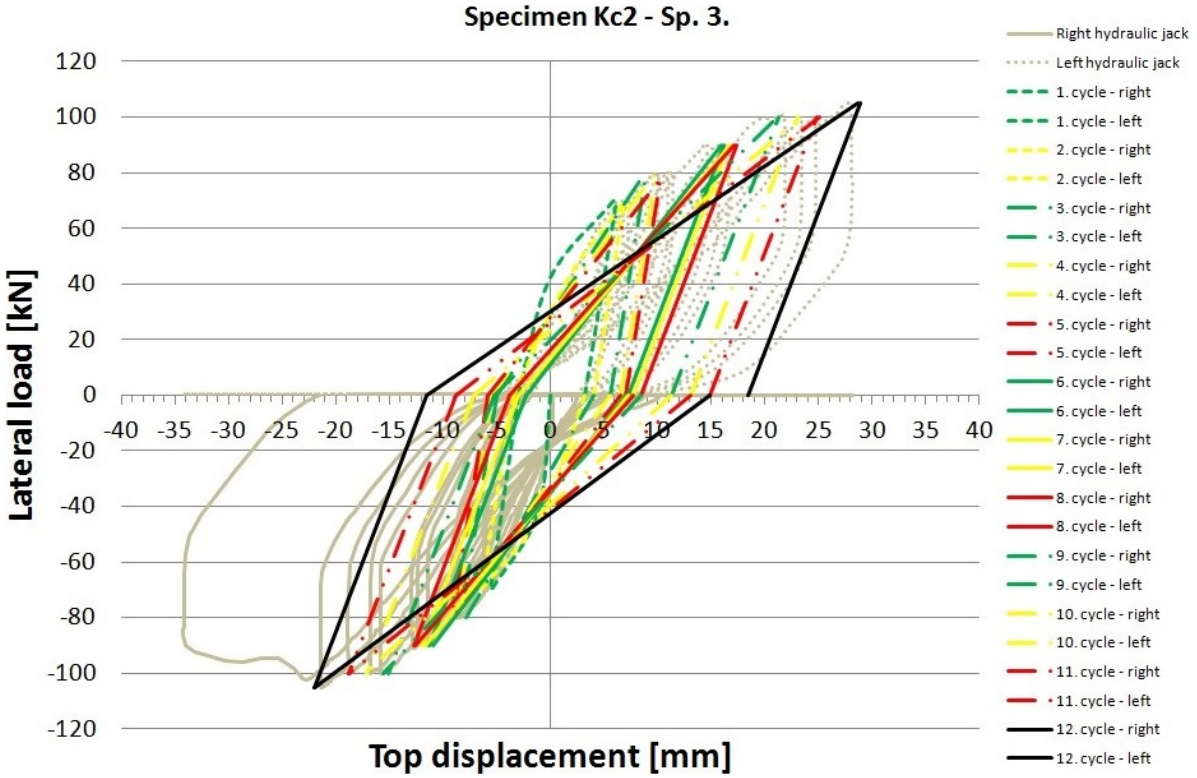

Fig. 24. Comparison of calculated and experimental results of Sp. Kc 2-3

Acknowledgement

The first author would like to express his grateful thanks to his supervisor, to prof. György Farkas for his persistant unselfish help.

The authors would like to express their grateful thanks to the colleagues in the Laboratory of the Budapest University of Technology and Economics.

References

1 *Eurocode 6 EN 1996-1-1:2009, Design of Masonry Structures*, 2009. European standard.

2 **Asteris PG**, *Lateral Stiffness of Brick Masonry Infilled Plane Frames*, Journal of Structural Engineering ASCE, **129(8)**, (2009), 1071–1079.

3 **Asteris PG**, *Finite Element Micro-Modeling of Unfilled Frames*, Int. Journal of the Physical Sciences, **2008(8)**, (2008), 1–11.

4 **Baran M, Sevil T**, *Analytical and Experimental Studies on Infilled RC Frames*, Int. Journal of the Physical Sciences, **5(13)**, (2010), 1981–1998.

5 **Bell DK, Davidson BJ**, *Evaluation of Earthquake Risk Buildings with Masonry Infill Panels*, In: New Zealand Society for Earthquake Engineering Inc. 2001 Conference, 2001, p. Paper No. 4.02.01.

6 **Braz-Cesar MT, Oliveira D, Barros RC**, *Comparison of Cyclic Response of Reinforced Concrete Infilled Frames with Experimental Results*, In: 14th World Conference on Earthquake Engineering; Beijing, China, October 12-17., 2008.

7 **Calvi MG, Bolognini D, Penna A**, *Seismic Performance of Masonry-Infilled RC Frames: Benefits of Slight Reinforcements*, In: SÍSMICA 2004-6°Congresso National de Sismologia e Engenharia Sísmica, 2004, pp. 253–276, http://www.civil.uminho.pt/masonry/Publications/Sismica_2004/253-276_G_Michele_Calvi.pdf.

8 **Dawe JL, Seah CK**, *Behaviour of masonry infilled steel frames*, Canadian Journal of Civil Engineerings, **16**(6), (1989), 865–876, DOI 10.1139/l89-129.

9 **Dincel B**, *The Roles of Masonry Infill Wall sin an Earthquake*, 2009, http://www.dincelconstructionsystem.com. Dincel Contruction System, Paramatta, Australia.

10 **Dulácska E**, *Földrengés elleni védelem, egyszerû tervezés az Eurocode 8 alapján. (Earthquake protection, simple design based on Eurocode 8)*, 2009. Practical guide, (in Hungarian).

11 **Hao H, Ma G-W, Lu Y**, *Damage assessment of masonry infilled RC frames subjected to blasting induced ground excitations*, Engineering Structures, **24**(2), (2002), 799–809, DOI 10.1016/S0141-0296(02)00010-X.

12 **Haris I, Hortobágyi Z**, *Modelling cast-in-situ reinforced concrete frame stiffened by masonry wall using FEM software*, Central Europen Congress on Concrete Engineering (Visegrád, Hungary, 17-18 September, 2007), In: Proceedings of CCC2007 (fib), 2007, pp. 469–474.

13 **Haris I, Hortobágyi Zs**, *Experimental research of masonry infilled frames for static load (in English translation)*, Concrete Structures (fib), **14**(1), (2012), 25–30. Budapest, Hungary,.

14 **Haris I, Hortobágyi Zs**, *Different FEM models of Reinforced Concrete Frames Stiffened by Infill Masonry for Lateral Loads*, Periodica Polytechnica Civil Engineering, **56**(1), (2012), 25–34, DOI 10.3311/pp.ci.2012-1.03.

15 **Haris I, Hortobágyi Zs**, *Comparison of experimental and analytical results on masonry infilled RC frames for monotonic increasing lateral load*, Periodica Polytechnica Civil Engineering, **56**(2), (2012), 185–196, DOI 10.3311/pp.ci.2012-2.05.

16 **Haris I**, *Experimental research of masonry infilled frames for cyclic load (in English translation)*, Concrete Structures (fib), **14**(4), (2012), 112–119. Budapest, Hungary.

17 **Haris I, Farkas G**, *Experimental results on masonry infilled RC frames for monotonic increasing and cyclic lateral load*, Structural Concrete (journal of the fib). under publication.

18 **Holmes M**, *Steel frames with brickwork and concrete infilling*, Institution of Civil Engineers (London, England, 1961), In: ICE Proceedings, Vol. 19, 1961, pp. 473–478, DOI 10.1680/iicep.1961.11305. E-ISSN: 1753-7789.

19 **Madan A, Reinhorn AM, Mander JB, Valles RE**, *Modeling of masonry infill panels for structural analysis*, Jounal of Structural Engineering, **123**(10), (1997), 1295–1302, DOI 10.1061/(ASCE)0733-9445(1997)123:10(1295).

20 **Magenes G, Pampanin S**, *Seismic Response of Gravity-load design frames with masonry infills*, 13th World Conference on Earthquake Engineering (Vancouver B.C. Canada, August 1-6., 2004), In: proceedings, 2004. Paper No. 4004.

21 **May IM**, *Determination of collapse loads for unreinforced panels with and without openings*, In: Proceedings of Instn. of Civil Engrs., Vol. 71; London, England, 1981, pp. 215–233, DOI 10.1680/iicep.1981.2149.

22 **Mehrabi AB, Shing PB, Schuller MP, Noland JL**, *Experimental Evaluation of masonry-infilled RC frames*, Journal of Structural Engineering (ASCE), **122**(3), (1996), 228–237, DOI 10.1061/(ASCE)0733-9445(1996)122:3(228). ISSN 07339445. ISBN 07339445.

23 **Murty CVR, Jain SK**, *Beneficial influence of masonry infill walls on seismic performance of rc frame buildings*, In: 12th World Conference on Earthquake Engineering; Auckland, New Zealand, January 30 – February 4., 2000.

24 **Lourenço PB, Alvaregna RC, Silva RM**, *Validation of a Simplified Model for the Design of Masonry Infilled Frames*, Masonry International, (2006), 15–26. ISSN 0950-2289. 19:1.

25 **Perera R**, *Performance evaluation of masonry-infilled RC frames under cyclic loading based on damage mechanics*, Engineering Structures, **27**, (2005), 1278–1288, DOI 10.1016/j.engstruct.2005.03.012.

26 **Polyakov SV**, *Masonry in Framed Buildings; An Investigations into the Strength and Stiffness of Masonry Infilling*, (1957). Moscow (In English translation).

27 **Puglisi M, Uzcategui M, López JF**, *Modelling of masonry of infilled frames, Part I: The Plastic Concentrator*, Elsevier Engineering Structures, **31**, (2009), 113–118, DOI 10.1016/j.engstruct.2008.07.012.

28 **Puyol S, Benavent-Client A, Rodriguez ME, Smith-Pardo JP**, *Masonry Infill Walls: An Effective Alternative for Seismic Strengthening of Low-rise Reinforced Concrete Building Structures*, In: 14th World Conference on Earthquake Engineering; Beijing, China, October 12-17., 2008.

29 **Saneinejad A, Hobbs B**, *Inelastic Design of Infilled Frames*, Journal of Structural Engineering, **121**(4), (1995), DOI 10.1061/(ASCE)0733-9445(1995)121:4(634). Paper No. 6682.

30 **Seah CK**, *Universal Approach for the Analysis and Design of Masonry-infilled Frame Structures*, PhD. Thesis, University of New Brunswick; Canada, 1998.

31 **Shing PB, Mehrabi AB**, *Behaviour and Analysis of Masonry-infilled Frames*, Progress in Structural Engineering and Materials, **4**(3), (2002), 320–331, DOI 10.1002/pse.122.

32 **Smith SB**, *Lateral stiffness of infilled frames*, Journal of the Structural Division, ASCE, **88**, (1962), 183–199.

33 **Smith SB**, *Behaviour of square infilled frames*, Journal of the Structural Division, ASCE, **92**, (1966), 381–403.

34 **Smith SB, Carter C**, *A method of analysis for infilled frames*, In:, pp. 31–48, DOI 10.1680/iicep.1969.7290. E-ISSN: 1753-7789.

35 **Tasnimi AA, Mohebkhah A**, *Investigation on the behaviour of brick infilled steel frames with openings, experimental and analytical approaches*, Engineering Structures, **33**(3), (2011), 968–980, DOI 10.1016/j.engstruct.2010.12.018.

36 **Wood RH**, *Plastic composite action and collapse design of unreinforced shear wall panels in frames*, In: Proceedings of Instn. of Civil Engrs., Vol. 65; London, England, 1978, pp. 381–411, DOI 10.1680/iicep.1978.2952.